Ann Nucl Med (2007) 21:577–584
DOI 10.1007/s12149-007-0071-6

ORIGINAL ARTICLE

Semi-quantitation of pulmonary perfusion heterogeneity on respiratory-gated inspiratory and expiratory perfusion SPECT in patients with pulmonary emphysema

Yasuhiko Kawakami · Kazuyoshi Suga
Mohammed Zaki · Hideyuki Iwanaga
Tomio Yamashita · Noriko Hayashi
Naofumi Matsunaga

Received: 26 February 2007 / Accepted: 3 September 2007

Abstract
Objective Pulmonary perfusion heterogeneity (PPH) in pulmonary emphysema (PE) was semi-quantified by functional lung volume rate (FLVR) curves obtained from respiratory-gated inspiratory and expiratory single-photon emission computed tomography (SPECT).
Methods Gated and ungated SPECT were obtained in 36 PE patients [25 with stage IIA and 11 with stage IIB for global initiative for chronic obstructive lung disease (GOLD) stage classification] and 12 controls, using a triple-head SPECT system and a respiratory tracking device. On gated SPECT, the voxel numbers calculated at the 10% cutoff threshold for the maximum lung radioactivity were assumed to be the functional lung volume of the lung (V). FLVR (%) was calculated as FLV divided by V at every additional 10% thresholds, yielding inspiratory and expiratory FLVR curves. The dissociations between these curves (ΔFLVRinsp – exsp) and the total difference (D index) of these curves from the normal standard curve (averaged inspiratory and expiratory curve in controls) were calculated. D index and the extent of low attenuation area (%LAA) on CT were correlated with the transfer coefficient for carbon monoxide (K_{CO}) in PE patients.
Results Although gated and ungated SPECT showed fairly uniform perfusion in controls, gated SPECT-enhanced PPH compared with ungated SPECT in PE patients, with significantly higher dissociation (ΔFLVRinsp – exsp) than that in controls (24.9% ± 9.5% vs. 4.5% ± 1.3%; $P < 0.0001$). ΔFLVRinsp – exsp was significantly higher even in stage IIA patients ($P < 0.0001$). Expiratory D index was significantly higher than the inspiratory one in PE patients ($P < 0.01$). This index was significantly higher in stage IIB patients than in stage IIA patients (44.1% ± 19.0% vs. 29.4% ± 13.7%; $P < 0.05$), and was significantly correlated with K_{CO} ($R = 0.642$, $P < 0.0001$) in all PE patients, although %LAA was not correlated with K_{CO}.
Conclusions FLVR curve analysis on gated SPECT appears useful for semi-quantitation of respiratory change of PPH in PE. Expiratory D index may better reflect the lung pathophysiology of PE than morphologic CT.

Keywords Single-photon emission computed tomography (SPECT) · Gated image · Lung perfusion · Pulmonary emphysema · Computed tomography (CT)

Introduction

Quantitation of pulmonary perfusion heterogeneity (PPH) on lung perfusion single-photon emission computed tomography (SPECT) with Tc-99m-macroaggregated albumin (Tc-99m-MAA) contributes to objective assessment of the severity of functional impairment in pulmonary emphysema (PE) [1–5]. An analysis of the functional lung volume rate (FLVR) curves, which are obtained in the lung segmentation process with various

Y. Kawakami · K. Suga (✉)
Department of Radiology, Semui Cancer Screening and Radiotherapy Site, St. Hill Hospital, 1462-3 Nishikiwa, Ube 755-0151, Japan
e-mail: sugar@sthill-hp.or.jp

M. Zaki · H. Iwanaga · T. Yamashita · N. Hayashi · N. Matsunaga
Department of Radiology, Yamaguchi University School of Medicine, Ube, Japan

cutoff thresholds on perfusion SPECT, has been proposed as one of the methods for the quantitation of PPH in PE [1]. However, FLVR curve analysis on conventional SPECT may underestimate PPH in PE, because respiratory lung motion and cyclically varying lung volume changes during image acquisition inherently obscure small/ill-defined perfusion defects [6–8].

The recently developed, respiratory-gated perfusion SPECT can reduce such adverse respiratory lung motion effects on conventional SPECT [8–11]. This gated SPECT also provides inspiratory and expiratory SPECT. FLVR curve analysis on these two SPECT may contribute to semi-quantitation of respiratory change of PPH in PE because the degree of PPH should be significantly changed according to respiratory lung volume changes [4, 5, 11]. In this study, we validated the utility of FLVR curve analysis on gated SPECT in the semi-quantitative assessment of PPH in PE patients.

Materials and methods

Study population

The subjects were 36 PE patients and 12 non-smoker controls with age closely matched with that of PE patients (Table 1), who had successfully undergone respiratory-gated perfusion SPECT during the period between November 2002 and July 2006. All subjects also underwent CT scan of the lung within 7 days of SPECT study. CT scan was performed at deep inspiratory breath-hold, using the multidetector row CT scanner with four rows of a 0.5 mm detector (Siemens Volume Zoom, Siemens-Asahi Medical, Tokyo, Japan). With the subject in the supine position, 3 mm-thick CT images covering the entire lungs were obtained in a 512 × 512 matrix during deep inspiratory breath-hold, using 3-mm collimation, with a tube rotation time of 1.0 s, at 120–135 kV_p and 200–230 mA. Transaxial CT images were reconstructed with the lung algorithm. The diagnosis of PE was made on physiologic findings, respiratory functional test, the presence of various extents of abnormal low attenuation area (LAA) of less than –910 Hounsfield units (HU) indicative of emphysematous lungs on CT, and cigarette smoking history (Table 1) [12, 13]. From the finding on CT, the pathologic type of emphysema was assumed to be centrilobular in 31 patients, panlobular in 3 patients, and undetermined in the remaining 1 patient. All these patients had only scattered, small bullae of less than 2 cm, which were preferentially present in the lung apex. According to the global initiative for chronic obstructive lung disease (GOLD) stage classification [14], 25 patients were stage IIA, and 11 patients were stage IIB. None of the controls had noticeable LAA on CT, with normal respiratory lung function test (Table 1). The procedure of respiratory-gated perfusion SPECT was approved by the Institutional Review Board of the Yamaguchi University School of Medicine. After the nature of the procedure had been fully explained, an informed consent was obtained from all subjects.

Table 1 Study population and lung function

PE patients	
Sex	32 males and 4 females
Age	61.2 ± 5.2 years (range 42–76 years)
Smoking history	26 ± 14 pack–years (range 12–90)
$\%FEV_1$	58.4% ± 10.3% (range 42.7%–74.5%)
%VC	81.6% ± 10.2% (range 82.4%–115.4%)
K_{CO}	3.3 ± 0.7 (range 2.1–4.9)
Healthy non-smokers	
Sex	12 females
Age	57.2 ± 4.3 years (range 46–78 years)
$\%FEV_1$	98.4% ± 3.2% (range 95.7%–111.7%)
%VC	95.8% ± 5.7% (range 92.7%–108.5%)
K_{CO}	5.6 ± 0.2 (range 5.1–5.8)

$\%FEV_1$ Predicted forced expiratory volume in 1 s, *%VC* predicted vital capacity, *K_{CO}* pulmonary transfer coefficient for carbon monoxide (the ratio of diffusing capacity of the lungs for carbon monoxide against alveolar volume)

Respiratory-gated perfusion SPECT

Respiratory-gated perfusion SPECT was performed using a triple-head SPECT system (GCA 9300 A/PI, Toshiba Medical System, Shibaura, Japan) equipped with low-energy high-resolution collimators and a laser light respiration-tracking device (AZ-733, Anzai Sogyo, Osaka, Japan). With each subject in the supine position, a 259 MBq (7 mCi) dosage of Tc-99m-MAA greater than the routine dosage of 111–148 MBq (3–4 mCi) was intravenously injected during several rest breathings to partly compensate for reduced lung radioactivity on gated images. However, the administered 0.18–0.2 mg MAA particles were the same as those in the routine dosage. Projection data were acquired using a stop and shoot mode, with 20 stops over 120° for each detector in a 64 × 64 matrix and pixel size of 6.4 mm, with an energy window of 140 keV ± 10%. A preset time of 15 s was set for each stop of 6°. The respiratory motion of each subject was monitored with time–distance curves on the respiration-tracking monitor, and any projection data of irregular respiratory cycles deviating beyond two standard deviations from the standardized cycle in each subject were automatically eliminated by the computer. Because the rejected projection data of irregular respira-

tory cycles were not counted toward 15 s for each stop of 6°, total image acquisition time varied according to the respiratory status of each patient, ranging from 8 to 14 min (mean 10.4 min ± 1.7 min).

On the image workstation (GCA 9300 A/DI, Toshiba Medical System), gated inspiratory and expiratory SPECT were reconstructed from the 1/8 threshold data centered at peak inspiration and expiration for each regular respiratory cycle, respectively, with use of a Butterworth prefilter (order no. 8, cutoff frequency 0.25 cycles/cm) and ramp backprojection filter. Scatter and attenuation corrections were not performed. For comparison, ungated SPECT was also reconstructed from the full data for every respiratory cycle. A total of 37–53 transaxial planes of each SPECT covering the entire lungs were reconstructed with a slice thickness of 1 pixel (6.4 mm). The lung contour of each SPECT was drawn at the 10% cutoff threshold for the maximum lung radioactivity in each subject. For visual inspection of gated and ungated SPECT on the image monitor, the same window width and level were used.

Data analysis

Two experienced observers (K.S. and N.H.) evaluated the lung perfusion appearance on gated and ungated perfusion SPECT on the image viewer of the image workstation. The DICOM data of gated and ungated perfusion SPECT were also transferred to the personal computer with image processing and analysis program (Scion image, version b4.0.2) for creating FLVR curves. The FLVR curves in all subjects were created and analyzed by a nuclear medicine specialist (Y.K.), according to the earlier reported method [1]. Briefly, the voxel numbers calculated from inspiratory and expiratory SPECT at the 10% cutoff threshold for the maximum lung radioactivity were assumed to be the functional lung volume of the lung (V). The threshold width number (n) was then taken from 1 to 9 for every additional 10% threshold. For example, letting t be the threshold, the threshold number (n) is 1 for $10\% < t < 20\%$, 2 for $20\% < t < 30\%$, . . . , 9 for $90\% < t < 100\%$, successively. The FLVR (%) was calculated as FLV divided by V at every additional 10% threshold; which yielded FLVR curves on inspiratory and expiratory SPECT. The total difference of FLVR (%) between inspiratory and expiratory FLVR curves (ΔFLVRinsp – exsp; %) on gated inspiratory and expiratory SPECT was estimated and compared with stage IIA and stage IIB PE patients and controls.

As the normal standard FLVR curve, the averaged curve obtained from inspiratory and expiratory SPECT images in healthy non-smokers was obtained. The total difference (D index; $\sum_{n=1}^{n=9}\left|\mathrm{FLVR}_n - \mathrm{FLVR}_n^{control}\right|$) of inspiratory and expiratory FLVR curves from this normal standard curve was calculated as an indicator of PPH in PE patients. As PPH increases, a shift of FLVR curve from the normal standard curve should be increased, resulting in a higher D index [10]. The D index was compared with stage IIA and stage IIB PE patients. This index was also correlated with pulmonary transfer coefficient for carbon monoxide (K_{CO}; the ratio of the diffusing capacity of the lungs for carbon monoxide against alveolar volume) as an indicator of alveolar-capillary destruction, to evaluate whether this index correctly reflects the lung pathophysiology in PE patients. K_{CO} was measured using the single-breath method (Pulmorecorder, model R1551S; Anima, Tokyo, Japan) according to the recommendation of the American Thoracic Society [12].

In addition to this FLVR curve analysis, to evaluate the extent of emphysematous changes on morphologic CT in PE patients, density-mask CT, which highlighted the lung areas with low attenuation values of less than –910 HU as red color areas, was created using imaging software (M900 QUADRA, Zio Soft K.K., Osaka, Japan) [15, 16]. The cutoff thresholds of –600 to –1024 HU were applied to segment the entire lungs and exclude soft tissues surrounding the lung and large vessels within the lungs. On the image viewer, the two observers (K.S. and N.H.) made a consensus reading for the relationship of perfusion defects on SPECT and LAA on density-mask CT in PE patients. In this assessment, the series of these SPECT and CT images were displayed side-by-side on the image viewer, and an adequate correspondence of each slice was confirmed by comparing the slice geometry from the lung apex and diaphragm on CT and SPECT scout view images, and by referring to the contours of the mediastinal and hilar structures. The extent of emphysematous changes on density-mask CT was quantified using the ratio of the number of voxels with LAA to the total numbers of voxels of the entire lungs (%LAA) [15, 16], and %LAA was also correlated with K_{CO} in PE patients.

Statistical analysis

Values were expressed as mean ± standard deviation (SD), and a paired or unpaired Student's t test was used for data comparison. A P value less than 0.05 was considered to be significant. A linear regression analysis was performed to evaluate the correlations of the D index or %LAA with K_{CO} in PE patients, with a P value less than 0.05 considered to be significant for each correlation coefficient (R).

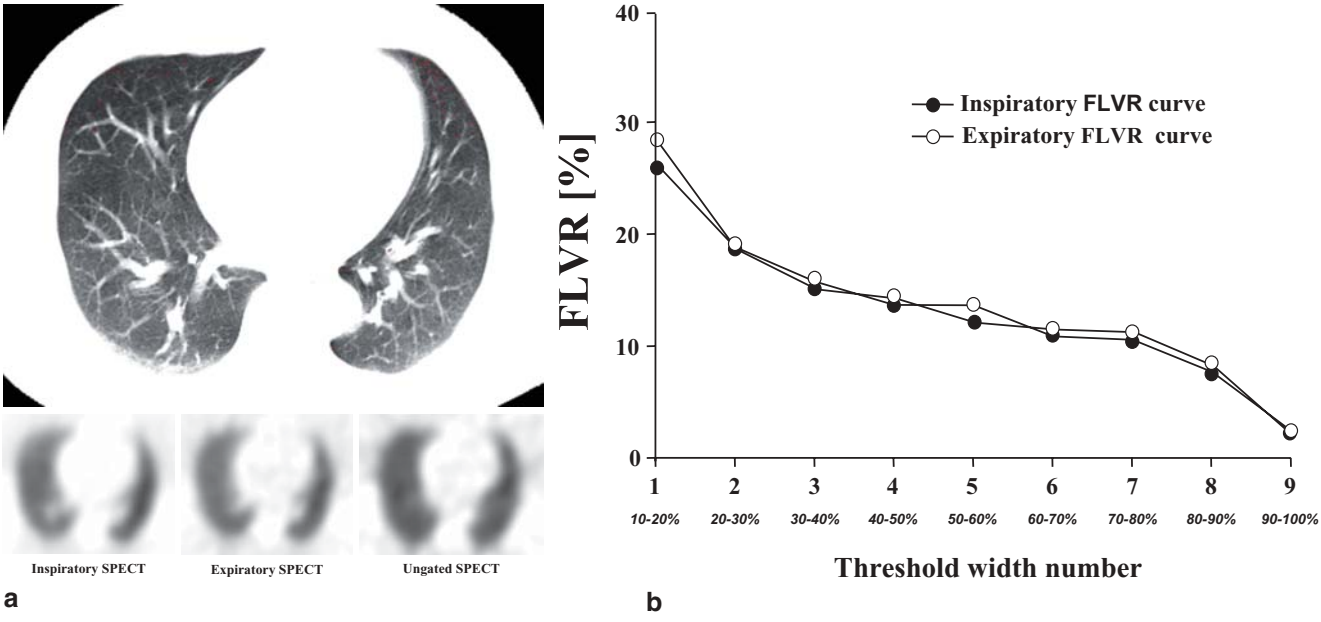

Fig. 1 A 53-year-old female healthy non-smoker. **a** Transaxial density-mask computed tomography (CT, *top*) shows no noticeable low-attenuation areas (LAA) of less than –910 HU in the lungs. Both inspiratory and expiratory perfusion single-photon emission computed tomography (SPECT; *bottom*, transaxial planes at almost the same lung level as density-mask CT) show fairly uniform perfusion, as well as ungated SPECT. **b** Inspiratory and expiratory functional lung volume rate (FLVR) curves show a similar pattern, with only a minimal dissociation

Results

In controls, all the ungated and gated SPECT showed fairly uniform perfusion. Inspiratory and expiratory FLVR curves showed only minimal dissociations, with ΔFLVRinsp – exsp of 4.5% ± 1.3% (range 2.6%–7.3%; Fig. 1). Density-mask CT showed no noticeable LAA throughout the lungs.

In PE patients, gated SPECT-enhanced PPH compared with ungated SPECT, and showed alteration of PPH between inspiratory and expiratory SPECT. The inspiratory and expiratory FLVR curves showed different patterns from those in controls, with various degrees of dissociations between these curves (Figs. 2, 3). Even in stage IIA patients, the dissociations (ΔFLVRinsp – exsp) were significantly higher than those in controls ($P < 0.0001$; Fig. 4). These values in stage IIB patients were significantly higher than those in stage IIA patients ($P < 0.001$). Overall, the mean ΔFLVRinsp – exsp of 24.9% ± 9.5% in all PE patients was significantly higher than that in controls ($P < 0.0001$), and this value in each patient persistently exceeded the value of 2 SD + the mean value in controls (7.1%).

Expiratory *D* index was significantly higher compared with inspiratory *D* index in PE patients (36.2% ± 15.9% vs. 26.4% ± 13.4%; $P < 0.01$). This index was significantly higher in stage IIB patients than in stage IIA patients (44.1% ± 19.0 vs. 29.4% ± 13.7%; $P < 0.05$), and was inversely correlated with K_{CO} ($R = 0.642$, $P < 0.0001$) in all PE patients (Fig. 5).

Density-mask CT showed various degrees of LAA in PE patients, with %LAA of 6.2% ± 4.7% (range 1.5%–22.1%). Perfusion defects on gated SPECT images were frequently seen even in the lung areas with only slight LAA or without LAA. Although %LAA was significantly higher in stage IIB patients than in stage IIA patients (25.3% ± 6.3% vs. 7.4% ± 2.9%; $P < 0.0001$), this value did not show a significant correlation with K_{CO} in any PE patients (Fig. 6).

Discussion

The present gated perfusion SPECT-enhanced PPH in PE patients compared with ungated SPECT, and showed respiratory alterations of PPH. FLVR curves on gated SPECT in these patients showed different patterns from those in controls, with significantly higher dissociations between inspiratory and expiratory curves (ΔFLVRinsp – exsp). ΔFLVRinsp – exsp was significantly higher even in stage IIA patients. Expiratory *D* index was significantly higher than inspiratory *D* index and showed a close correlation with K_{CO} in these patients, although the degree of extent of emphysematous lungs (%LAA) on CT did not show a significant correlation. FLVR curve analysis with use of the parameter of ΔFLVRinsp – exsp

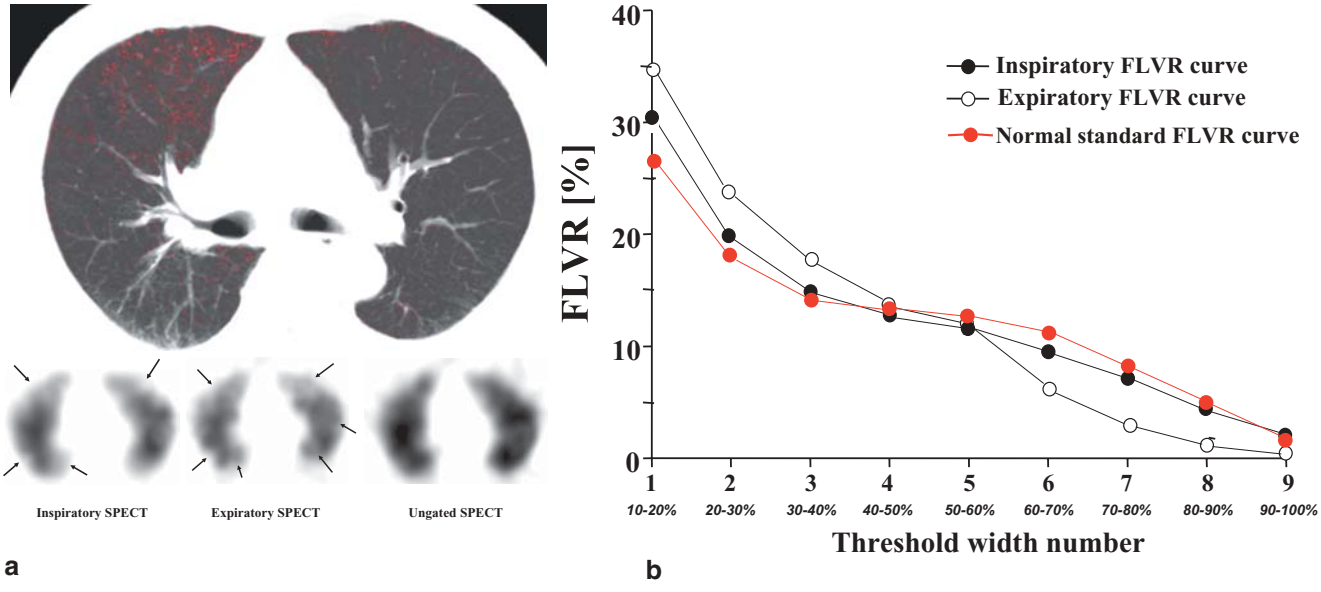

Fig. 2 A 52-year-old male patient with pulmonary emphysema (PE) and Brinkman index (cigarette consumption per day × years) of 640. **a** Transaxial density-mask CT image (*top*) shows heterogeneous LAA of less than –910 HU (*red colors*) in both lungs, with the extent of LAA (%LAA) of 4.9%. Gated and ungated SPECT (*bottom*; transaxial planes at almost the same lung level as density-mask CT) show heterogeneous perfusion defects, which appear to be more enhanced on gated SPECT (*arrows*). Perfusion defects are seen even at the lung areas with only slight LAA in the left ventral lung. **b** Inspiratory and expiratory FLVR curves show a significant dissociation compared with those in controls presented in Fig. 1b. These curves also show a different pattern from the normal standard FLVR curve (the average FLVR curve of inspiratory and expiratory curves in 12 healthy non-smokers; *red line*). The dissociation from the normal standard FLVR curve is more prominent in the expiratory curve compared with that in the inspiratory curve

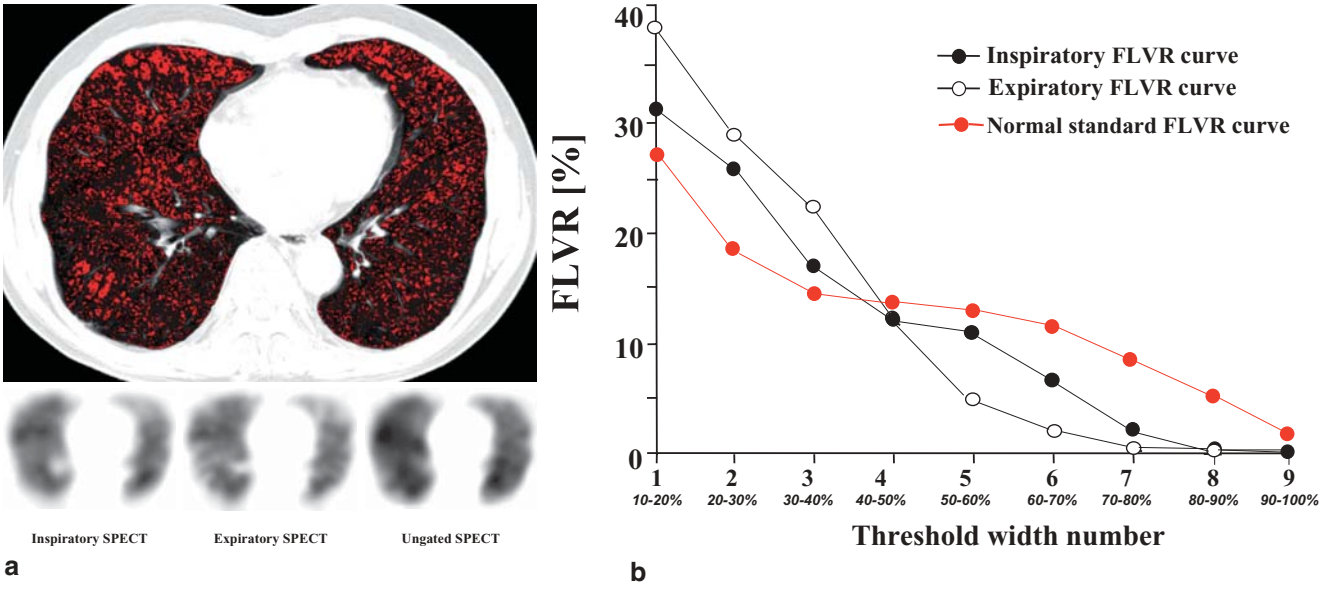

Fig. 3 A 65-year-old male PE patient with Brinkman index of 980. **a** Transaxial density-mask CT (*top*) shows widely distributed heterogeneous LAA of less than –910 HU (*red colors*), with %LAA of 34.0%. Gated and ungated SPECT (*bottom*; transaxial planes at almost the same lung level as density-mask CT) show heterogeneous perfusion defects, which appear to be more enhanced on gated SPECT. **b** Inspiratory and expiratory FLVR curves show marked dissociations compared with those in the patient with less pulmonary emphysematous changes presented in Fig. 2. The dissociation from the normal standard FLVR curve (*red line*) is more prominent in the expiratory curve compared with that in the inspiratory curve

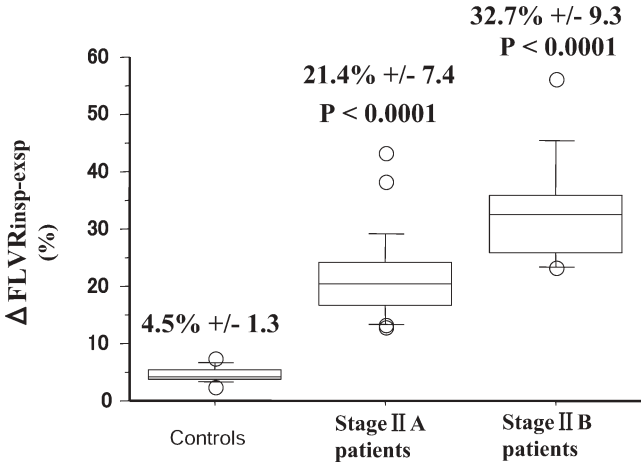

Fig. 4 Comparison of dissociations between gated inspiratory and expiratory FLVR curves (ΔFLVRinsp – exsp) among stage IIA and IIB PE patients and controls. ΔFLVRinsp – exsp of 21.4% ± 7.4% in stage IIA patients and that of 32.7% ± 9.3% in stage IIB patients are significantly higher than that of 4.5% ± 1.3% in controls (both; $P < 0.0001$). This value in stage IIB patients is significantly higher than that in stage IIA patients ($P < 0.001$)

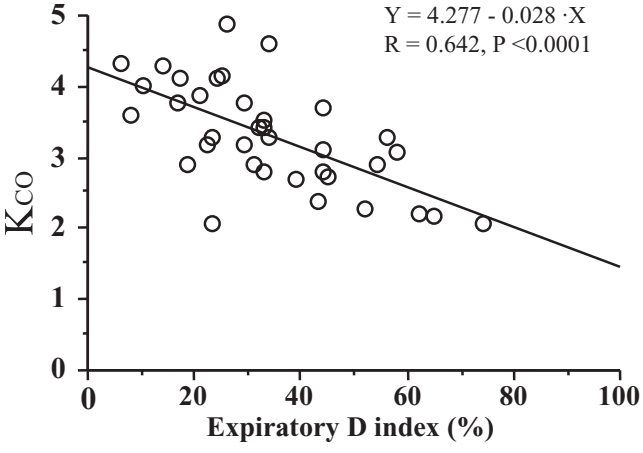

Fig. 5 Comparison of expiratory *D* index and pulmonary transfer coefficient for carbon monoxide (K_{CO}) in 36 PE patients. Expiratory *D* index is significantly and inversely correlated with K_{CO}, as $Y = 4.277 - 0.028X$; $R = 0.642$ ($P < 0.0001$)

on gated SPECT appears useful for semi-quantitation of respiratory change of PPH in PE. Expiratory *D* index may better reflect the lung pathophysiology of PE than morphologic CT.

Emphysematous lungs with alveolar destruction and smoking-induced airway pathology significantly impair lung perfusion [14–18]. The present gated SPECT better depicted PPH of emphysematous lungs compared with ungated SPECT. The enhanced PPH on gated SPECT is considered to be partly owing to the improvement of adverse respiratory lung motion effects [6–11]. In non-breath-hold SPECT, lung motion during every respiratory cycles and the cyclically changing lung volume inherently obscure PPH [6–11]. The enhanced PPH on gated SPECT is also explained by alteration of radioactivity per unit lung volume and the size of defects because of respiratory lung volume changes [6–11]. PPH should be significantly altered between inspiratory and expiratory SPECT in emphysematous lungs with heterogeneous air trapping [15–17,18–20]. The dissociations between inspiratory and expiratory FLVR curves (ΔFLVRinsp – exsp) in our PE patients can be explained by this alteration of PPH during respiration. In contrast, normal lungs show persistently uniform perfusion during respiration because of relatively uniform alveolar air space changes, resulting in only minimal dissociations [15, 16]. The dissociations seem to be prevalent even in PE patients with the relatively early stage of PE, as ΔFLVRinsp – exsp was significantly higher even in stage IIA patients compared with the controls. The dissociations also seem to be greater according to the progress of the stage of PE, as ΔFLVRinsp – exsp was significantly higher in stage IIB patients than in stage IIA patients.

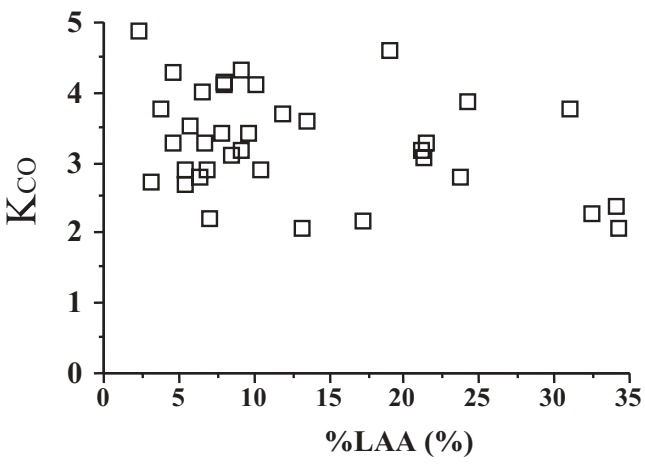

Fig. 6 Comparison of %LAA on density-mask CT and K_{CO} in 36 PE patients. There is no significant correlation between %LAA and K_{CO}

The expiratory *D* index seems to be a sensitive parameter in assessing PPH of emphysematous lungs, as this index was significantly higher than inspiratory *D* index in our PE patients. During expiration, the radioactivity per unit lung volume in emphysematous lung areas may not be significantly altered owing to the presence of air trapping, as the earlier expiratory CT studies showed reduced respiratory volume changes [19, 20]. In contrast, the radioactivity per unit lung volume in the surrounding normal lung areas should be significantly increased owing to significant reduction of alveolar air space during expiration, resulting in enhancement of PPH on

expiratory SPECT. The previous pulmonary embolic dog models using planar scintigrams showed better defect clarity of pulmonary perfusion defects on end-expiration image than on end-inspiration image [21]. In contrast, during inspiration, the difference of the radioactivity per unit lung volume between emphysematous and normal lung areas is reduced because these two areas uniformly expand during inspiration. Expiratory *D* index may be able to reflect the progress of the stage of PE, as this index was significantly higher in our IIB stage patients than in stage IIA patients. This index also seems to reflect the pathophysiology of emphysematous lungs, as indicated by the close correlation with K_{CO} in our patients. Although K_{CO} is a global indicator of the pathophysiology of emphysematous lungs, visualization of perfusion defects on gated SPECT is of value for localizing the sites of emphysematous lungs.

The present gated SPECT seems more sensitive in detecting the affected lungs than morphologic CT in PE patients, as perfusion defects were frequently seen even in the lung areas with minimal LAA on CT. The expiratory *D* index was also closely correlated with K_{CO} in our patients, although the extent of LAA on CT was not significantly correlated. CT has certain limitations in detecting emphysematous lungs because of limited spatial resolution [22–27]. The earlier clinical studies showed a relatively low prevalence of LAA on CT, regardless of significant airflow limitation in respiratory function test in PE patients [22, 24]. The earlier animal pathologic study also showed that a perfusion scintigram was more sensitive in detecting elastase-induced emphysema compared with CT [2]. Smoking-induced airway obstruction also may impair regional ventilation and result in lung perfusion defects regardless of the absence of emphysematous changes on CT [14–16, 25]. The extent of LAA on CT in PE patients also may largely vary during respiration [16, 19, 23, 27].

The present preliminary study indicates that FLVR curve analysis on gated SPECT may be very useful for objective semi-quantitation of PPH in PE. This analysis may be a useful adjunct to GOLD stage classification in determining the stage of PE and may contribute to follow-up assessment of the development of functional impairment in PE patients, as ΔFLVRinsp – exsp and expiratory *D* index were significantly different between our stage IIA and stage IIB patients. The drawback of this study is that the controls studied here included age-matched women alone. This might cause some bias for the pattern of the normal standard FLVR curve. The other drawback is that the PE patients studied here included only stage IIA and stage IIB patients for GOLD stage classification. It is unclear whether FLVR curve analysis on gated SPECT can sensitively detect at risk or mild stage PE patients. In patients with more advanced disease, the degree of PPH might be overestimated on gated SPECT because of reduced photon accumulation by gating image data acquisition, and respiratory change in PPH might be markedly reduced owing to extensively decreased lung volume changes. Further studies are warranted on these issues.

In conclusion, gated perfusion SPECT enhanced PPH compared with ungated SPECT in PE patients. FLVR curves on the inspiratory and expiratory SPECT in PE patients showed differences from those in controls. The dissociations between inspiratory and expiratory FLVR curves (ΔFLVRinsp – exsp) were significantly higher even in stage IIA patients. The expiratory *D* index was significantly higher than the inspiratory one, and this index was significantly higher in stage IIA patients than that in stage IIB patients, and overall showed a close correlation with K_{CO} in PE patients. However, the extent of LAA on CT in these patients did not show a significant correlation with K_{CO}. Although further validation is warranted, FLVR curve analysis on gated SPECT appears useful for objective semi-quantitation of respiratory change of PPH in PE. Expiratory *D* index may better reflect the lung pathophysiology of PE than morphologic CT.

References

1. Mitomo O, Aoki S, Tsunoda T, Yamaguchi M, Kuwabara H. Quantitative analysis of nonuniform distribution in lung perfusion scintigraphy. J Nucl Med 1998;39:1630–5.
2. Noma S, Moskowitz GW, Herman PG. Pulmonary scintigraphy in elastase-induced emphysema in pigs: correlation with high-resolution computed tomography and histology. Invest Radiol 1992;27:429–35.
3. Eidelmn D, Saetta M, Ghezzo H, Wang NS, Hoidal JR, King M. et al. Cellularity of the alveolar walls in smokers and its relation to alveolar destruction: functional implications. Am Rev Respir Dis 1990;140:1547–52.
4. Sando Y, Inoue T, Nagai R, Endo K. Ventilation/perfusion ratios and simultaneous dual-radionuclide single-photon emission tomography with krypton-81m and technetium-99m macroaggregated albumin. Eur J Nucl Med 1997;24: 1237–44.
5. Petersson J, Sanchez-Crespo A, Rohdin M, Montmerle S, Nyren S, Jacobsson H, et al. Physiological evaluation of a new quantitative SPECT method measuring regional ventilation and perfusion. J Appl Physiol 2004;96:1127–36.
6. Ketai L, Hartshorne M. Potential uses of computed tomography-SPECT and computed tomography-coincidence fusion images of the chest. Clin Nucl Med 2001;26:433–41.
7. Nehmeh SA, Erdi YE, Ling CC, Rosenzweig KE, Squire OD, Braban LE, et al. Effect of respiratory gating on reducing lung motion artifacts in PET imaging of lung cancer. Med Phys 2002;29:366–71.
8. Suga K. Technical and analytic advances in pulmonary ventilation SPECT with xenon-133 gas and Tc-99m-Technegas. Ann Nucl Med 2002;16:303–10.

9. Suga K, Kawakami Y, Zaki M, Yamashita T, Matsumoto T, Matsunaga N. Pulmonary perfusion assessment with respiratory gated Tc-99m-macroaggregated albumin SPECT: preliminary results. Nucl Med Commun 2004;25:183–93.
10. Suga K, Kawakami Y, Zaki M, Yamashita T, Seto A, Matsumoto T, et al. Assessment of regional lung functional impairment with co-registered respiratory-gated ventilation/perfusion SPET-CT images: initial experiences. Eur J Nucl Med Mol Imaging 2004;31:240–9.
11. Ue H, Haneishi H, Iwanaga H, Suga K. Nonlinear motion correction of respiratory-gated lung SPECT images. IEEE Trans Med Imaging 2006;25:486–95.
12. American Thoracic Society. Standards for the diagnosis and care of patients with chronic obstructive pulmonary disease. Am J Respir Crit Care Med 1995;152:S78–83.
13. Petty TL. COPD in perspective. Chest 2002;121:116S–20S.
14. Cosio MG, Hale KA, Niewoehner DE. Morphologic and morphometric effects of prolonged cigarette smoking on the small airways. Am Rev Respir Dis 1980;122:265–71.
15. Park KJ, Bergin CJ, Clausen JL. Quantitation of emphysema with three-dimensional CT densitometry: comparison with two-dimensional analysis, visual emphysema scores, and pulmonary function test results. Radiology 1999;211:541–7.
16. Kinsella M, Muller NL, Abboud RT, Morrison NJ, DyBuncio A. Quantitation of emphysema by computed tomography using a "density mask" program and correlation with pulmonary function tests. Chest 1990;97:315–21.
17. Lams BE, Sousa AR, Rees PJ, Lee TH. Immunopathology of the small-airway submucosa in smokers with and without chonic obstructive pulmonary disease. Am J Respir Crit Care Med 1998;158:1518–23.
18. Berger P, Laurent F, Begueret H, Perot V, Rouiller R, Raherison C, et al. Structure and function of small airways in smokers: relationship between air trapping at CT and airway inflammation. Radiology 2003;228;85–94.
19. Lamers RJ, Thelissen GR, Kessels AG, Wouters EF, van Engelshoven JM. Chronic obstructive pulmonary disease: evaluation with spirometrically controlled CT lung densitometry. Radiology 1994;193:109–13.
20. Knudson RJ, Standen JR, Kaltenborn WT, Knudson DE, Rehm K, Habib MP, et al. Expiratory computed tomography for assessment of suspected pulmonary emphysema. Chest 1991;99:1357–66.
21. Alderson PO, Vieras F, Housholder DF, Mendenhall KG, Wagner HN Jr. Gated and cinematic perfusion lung imaging in dogs with experimental pulmonary embolism. J Nucl Med 1979;20:407–12.
22. Fujita E, Nagasaka Y, Kozuka T, Ebara H, Fukuoka M. Correlation among the indices of high-resolution computed tomography, pulmonary function tests, pulmonary perfusion scans and exercise tolerance in cases of chronic pulmonary emphysema. Respiration 2002;69:30–7.
23. Gevenois PA, De Vuyst P, de Maertelaer V, Zanen J, Jacobovitz D, Cosio MG, et al. Comparison of computed density and microscopic morphometry in pulmonary emphysema. Am J Respir Crit Care Med 1996;154:187–92.
24. Remy-Jardin M, Remy J, Gosselin B, Copin MC, Wurtz A, Duhamel A. Sliding thin slab, minimum intensity projection technique in the diagnosis of emphysema: histopathologic-CT correlation. Radiology 1996;200:665–71.
25. Thurlbeck WM. Chronic airflow obstruction. In: Thurlbeck WM, editors. Pathology of the lung. New York: Thieme Medical;1998. p. 519–75.
26. Miller RP, Müller NL, Vedal S. Limitations of computed tomography in the assessment of emphysema. Am Rev Respir Dis 1989;139:980–3.
27. Kuwano K, Matsuba K, Ikeda T, Murakami J, Araki A, Shigematsu Nl. The diagnosis of mild emphysema: correlation of computed tomography and pathology scores. Am Rev Respir Dis 1990;141:169–78.